Electronic Supplementary Material (ESI) for Physical Chemistry Chemical Physics.

Electrochemical impedance spectroscopy reveals a new mechanism based on competitive binding between Tris and protein on a conductive biomimetic polydopamine surface

Nimisha Singh[#], Jyotsnamayee Nayak[#], Khushbu Patel, Suban K Sahoo and Rajender Kumar*

 # Contribution of Nimisha Singh and Jyotsnamayee is major and equal

[1*]Department of Applied Chemistry, S.V. National Institute of Technology, Surat-395007, Gujarat,India.

***Corresponding Author, E. mail:** rajenderkumar@chem.svnit.ac.in(RK); Ph.(O)-+91-261-2201655

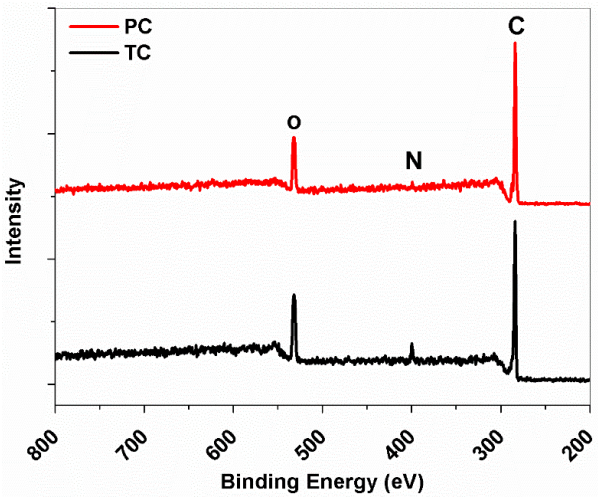

Figure S1: XPS survey scan of Polydopamine coatings prepared on gold wafer in Tris (TC) and PBS (PC) buffers respectively.

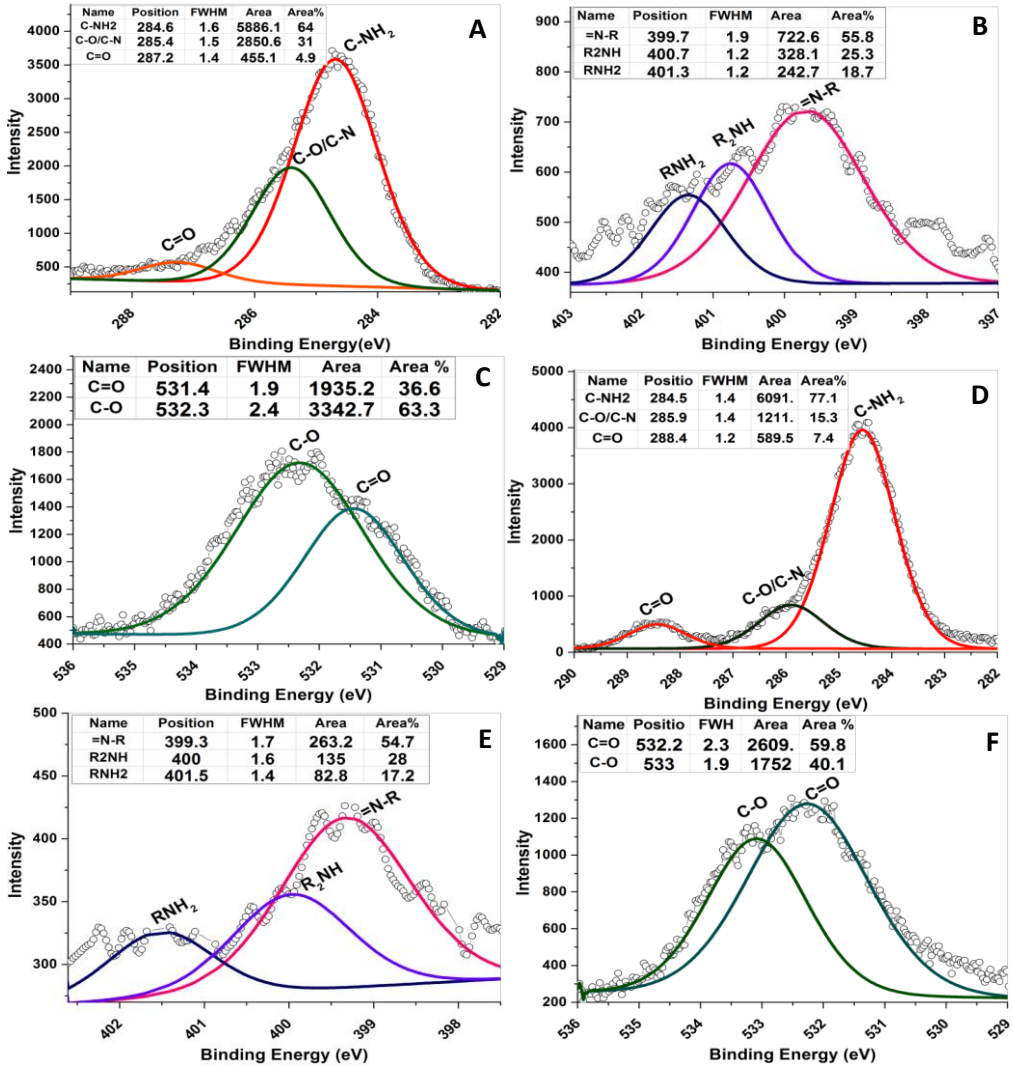

Figure S2: Deconvoluted XPS spectra of (A-C) C 1s, N 1s, and O 1s element in Tris buffer and (D-F) C 1s, N 1s, and O 1s element in PBS buffer for PDA coated gold wafer.

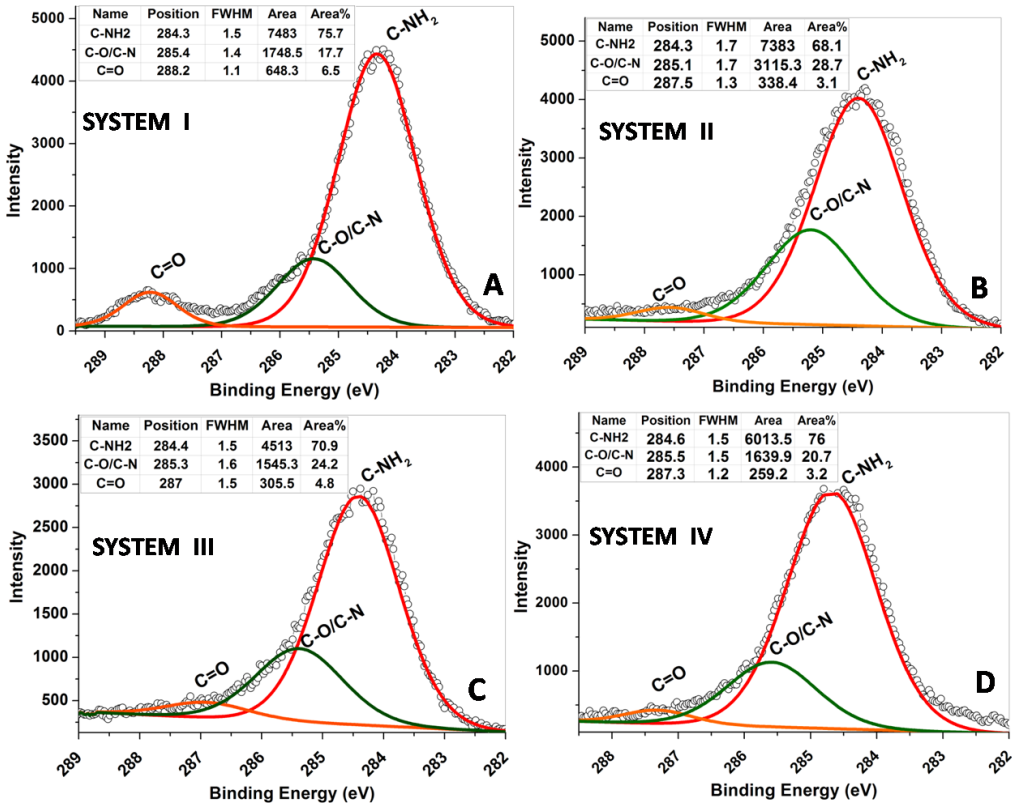

Figure S3: Deconvoluted spectra of C1s element showing PDA coated electrode in A. Tris coated gold electrode in Tris solution, B. Tris coated gold electrode in PBS solution, C. PBS Coated gold electrode in Tris solution and D. PBS coated gold electrode in PBS solution.

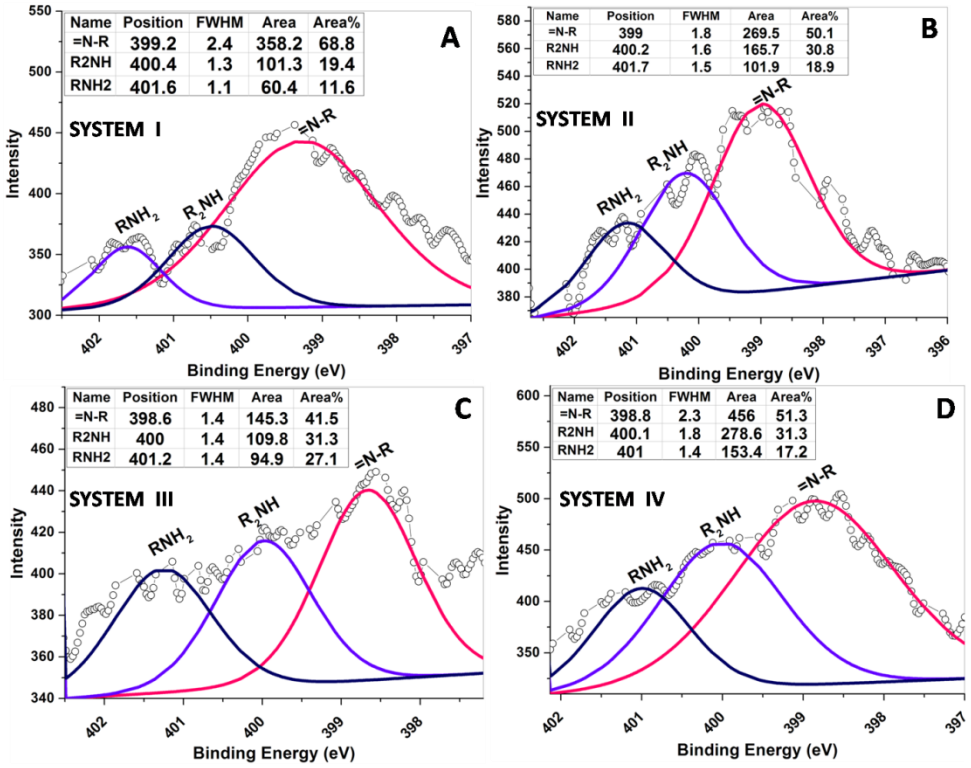

Figure S4:Deconvoluted spectra of N1s element showing PDA coated electrode in A. Tris coated gold electrode in tris solution, B. Tris coated gold electrode in PBS solution, C. PBS Coated gold electrode in Tris solution and D. PBS coated gold electrode in PBS solution bonded with BSA protein.

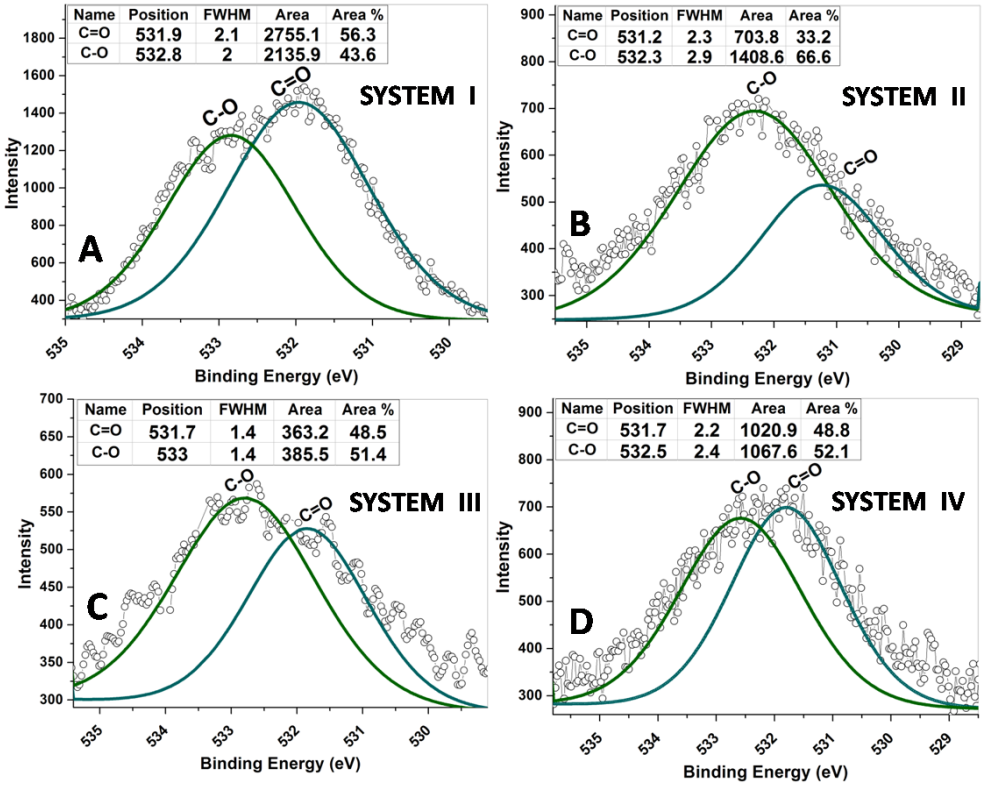

Figure S5: Deconvoluted spectra of O1s element showing PDA coated electrode in A. Tris coated gold electrode in Tris solution, B. Tris coated gold electrode in PBS solution, C. PBS Coated gold electrode in Tris solution and D. PBS coated gold electrode in PBS solution bonded with BSA protein.

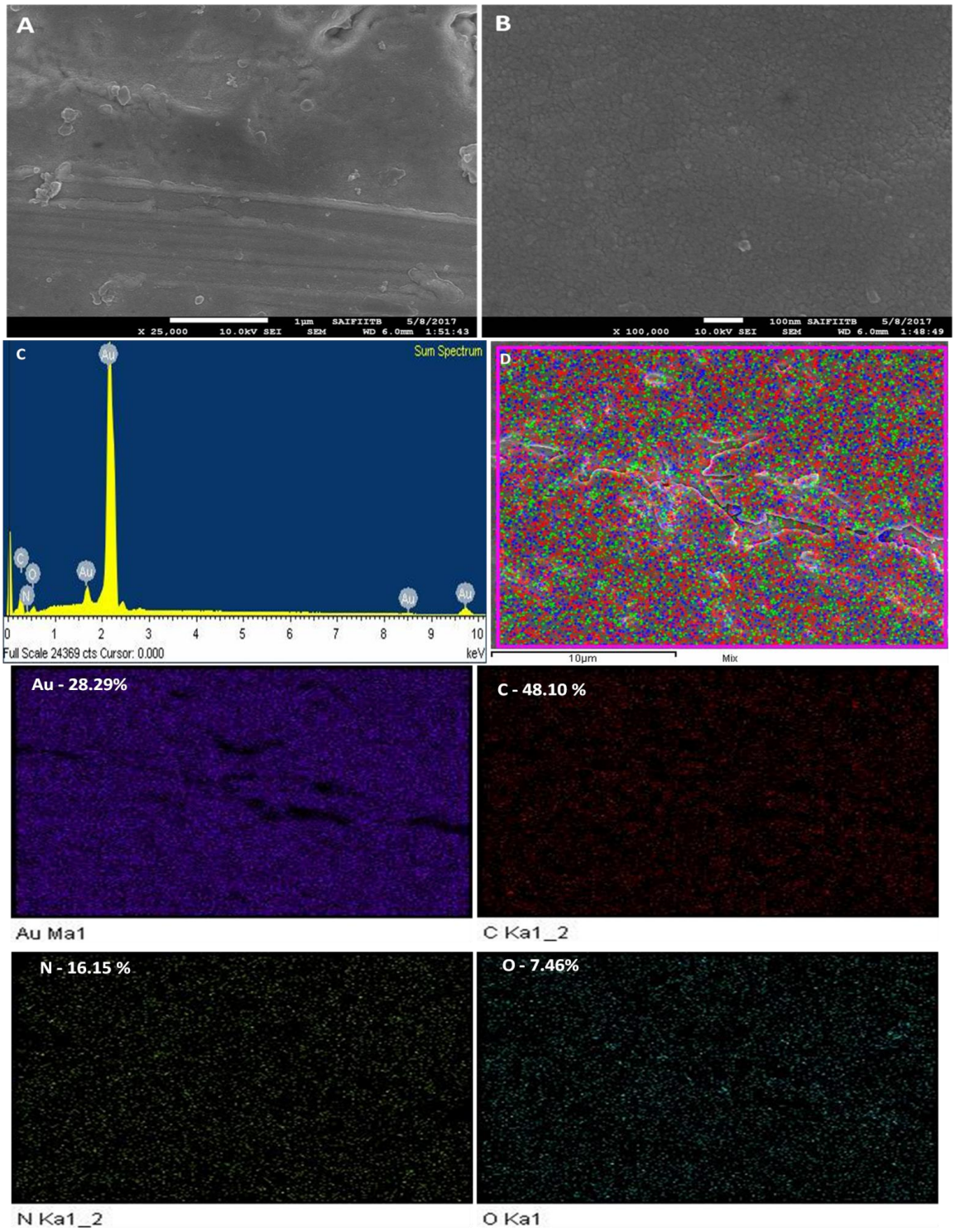

Figure S6: (A-B) SEM images of Tris-PDA electrode, C. EDS spectra and D. Elemental mapping showing the percentage of elements present on Au wafer.

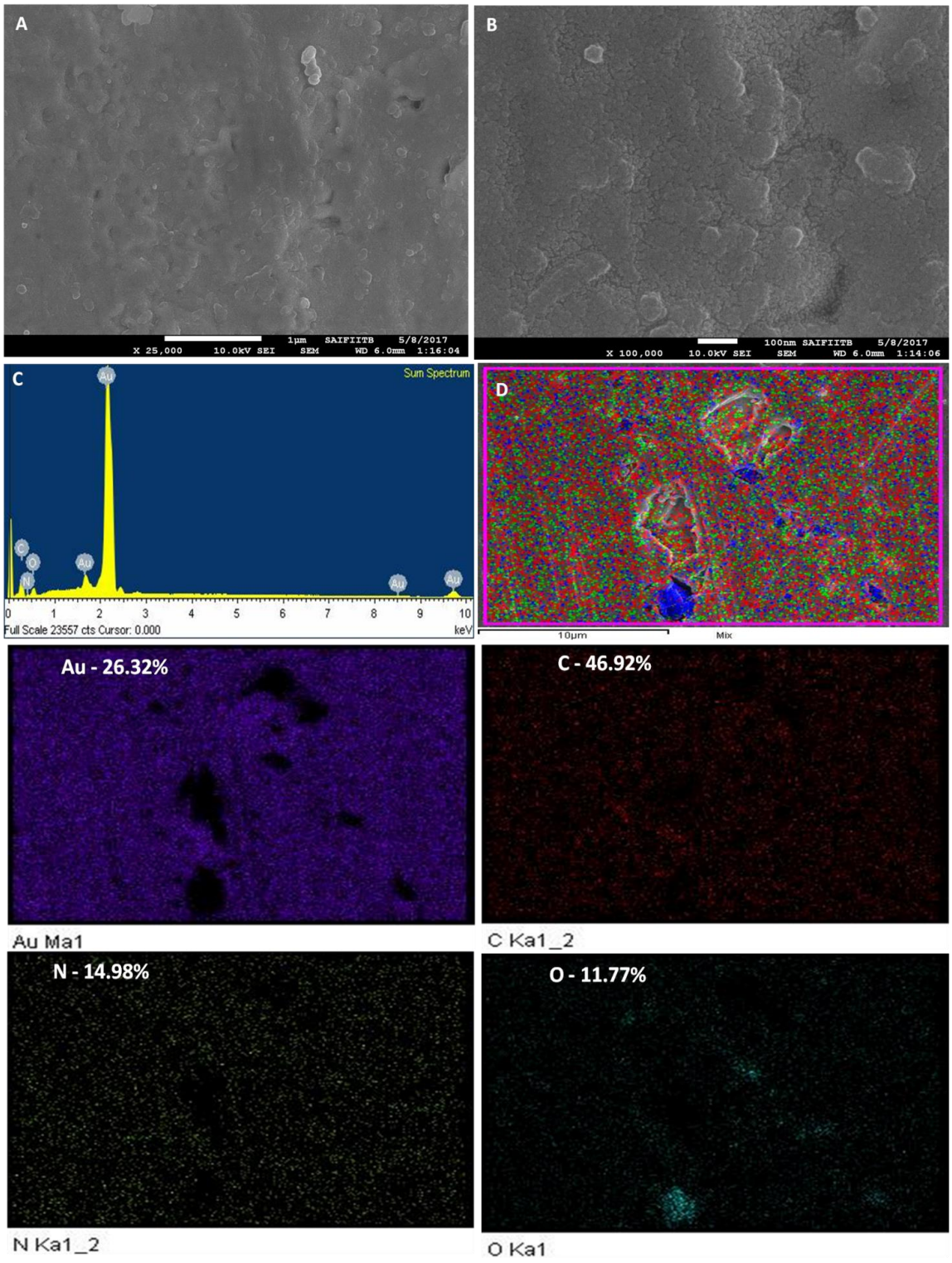

Figure S7: (A-B) SEM images of PBS-PDA electrode, C. EDS spectra and D. Elemental mapping showing the percentage of elements present on Au wafer.

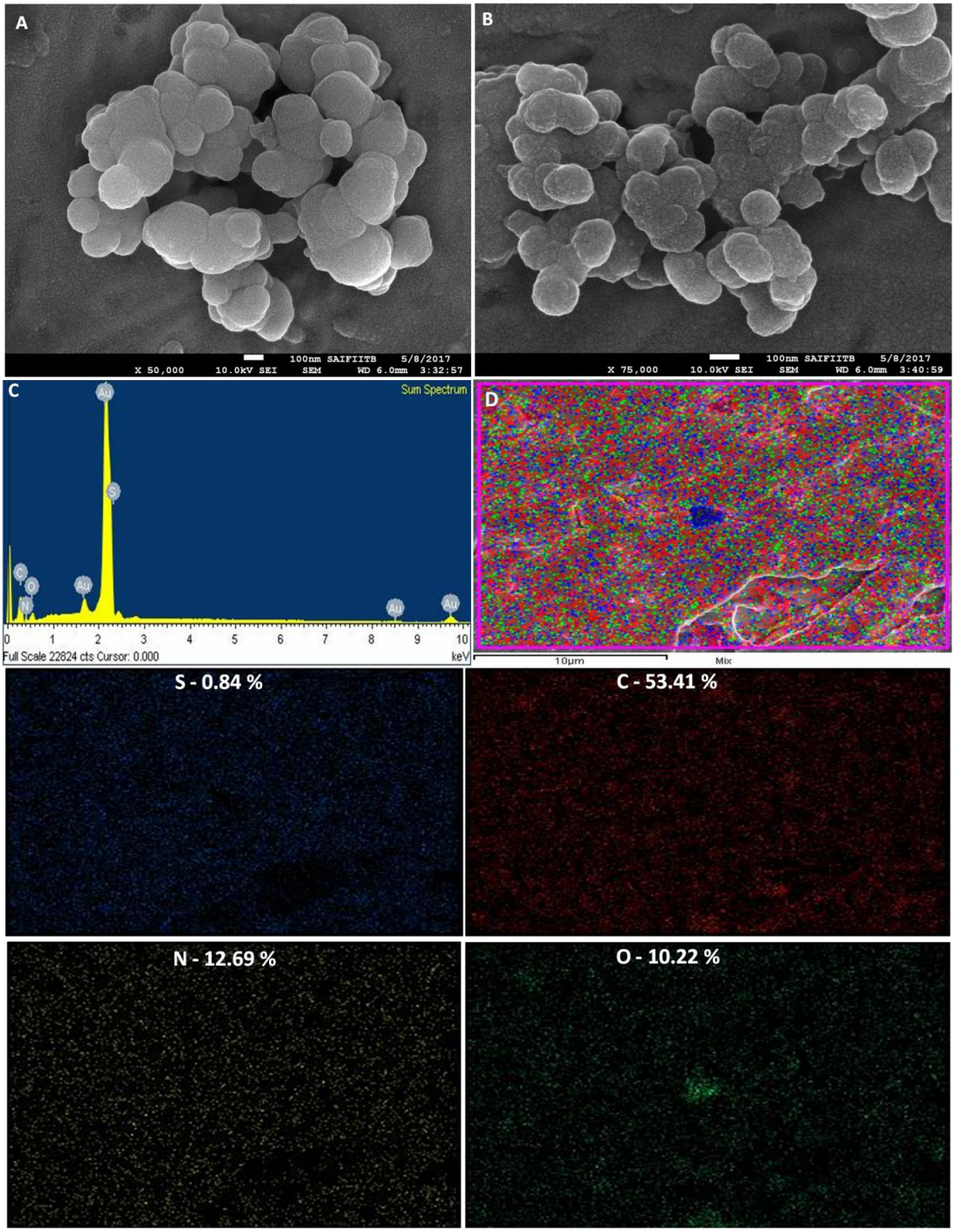

Figure S8: (A-B) SEM images of PBS-PDA electrode with Protein in PBS buffer (System IV), C. EDS spectra and D. Elemental mapping showing the percentage of elements present on Au wafer.

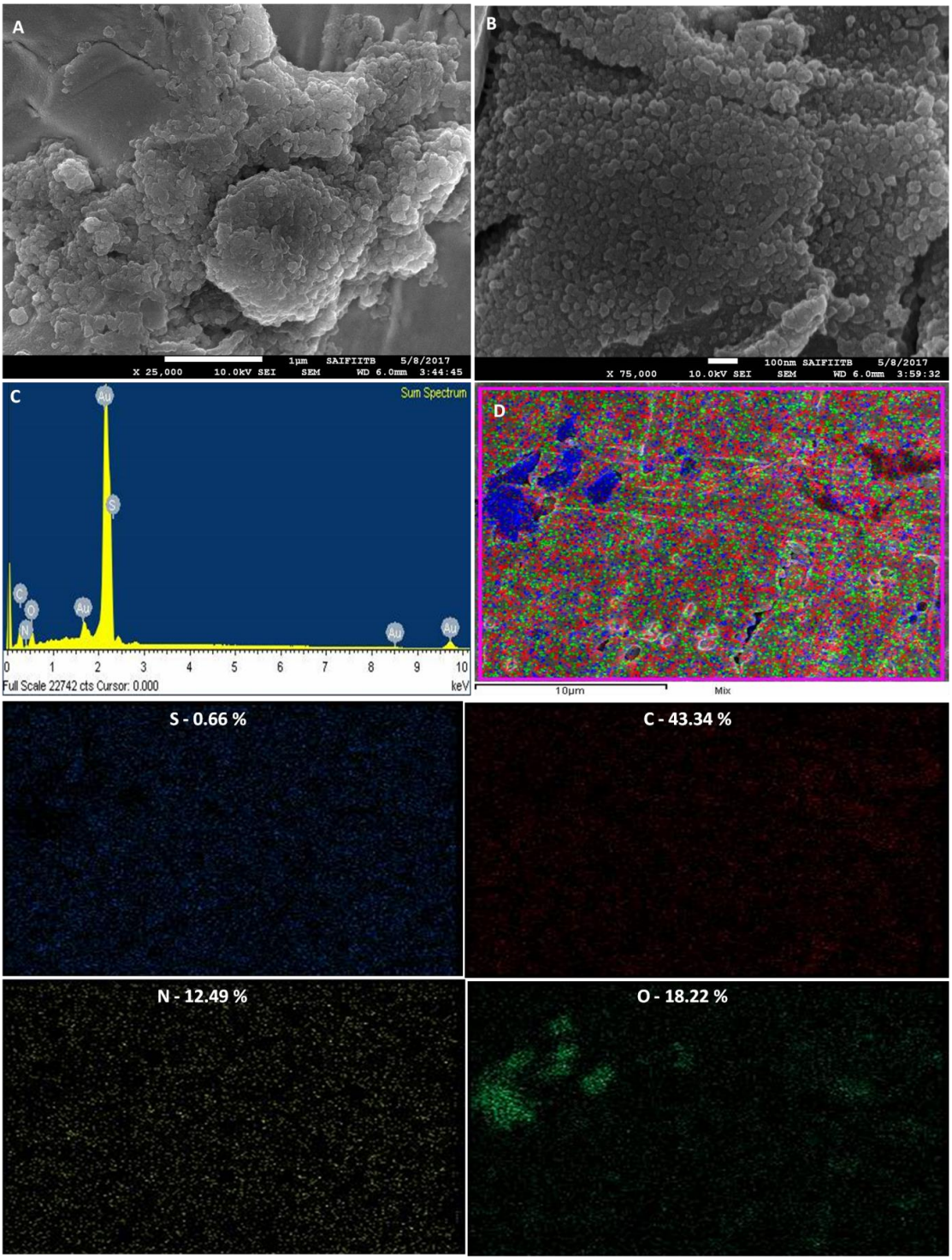

Figure S9: (A-B) SEM images of PBS-PDA electrode with Protein in Tris buffer(System III), C. EDS spectra and D. Elemental mapping showing the percentage of elements present on Au wafer.

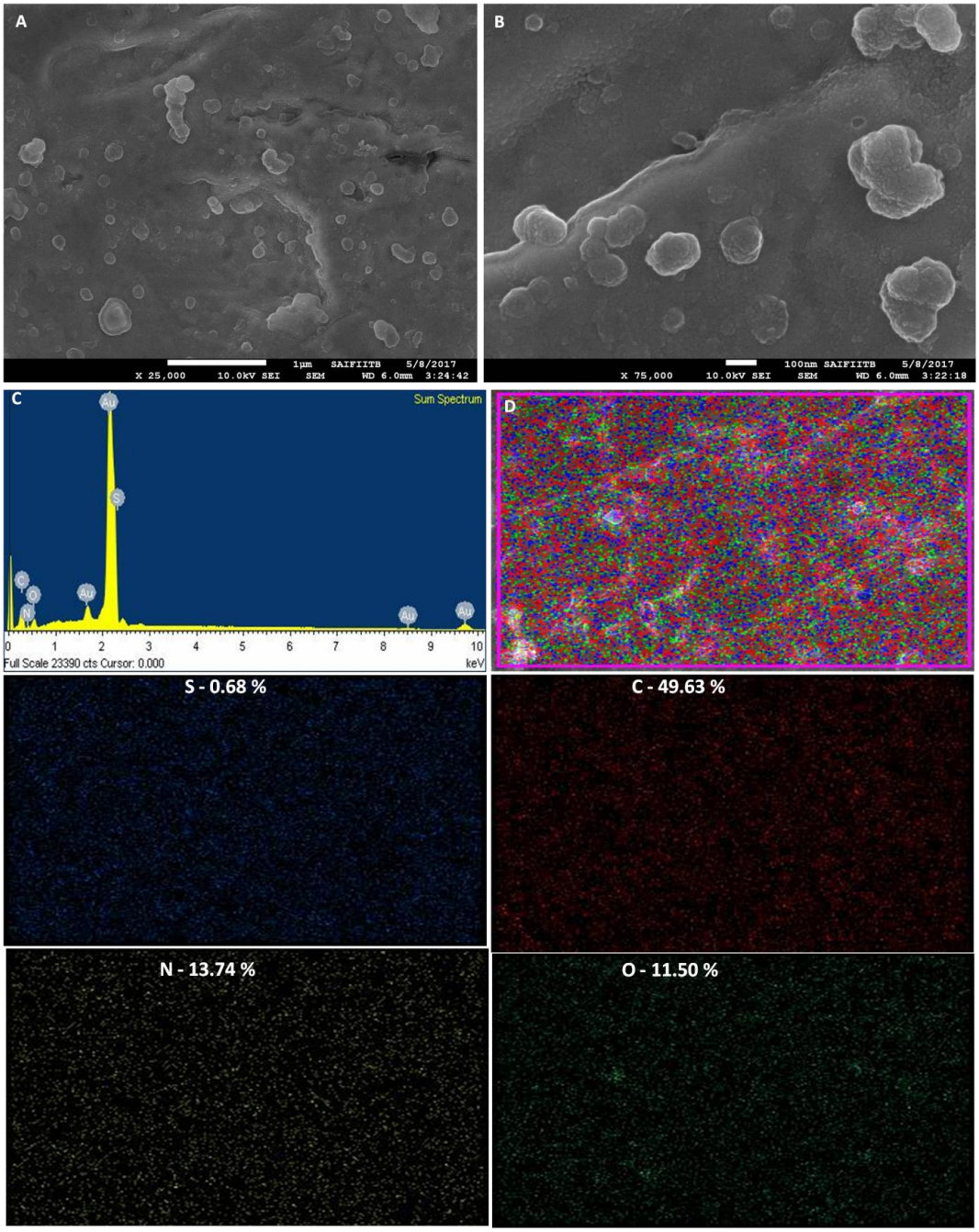

Figure S10: (A-B) SEM images of Tris-PDA electrode with Protein in Tris buffer (System I), C. EDS spectra and D. Elemental mapping showing the percentage of elements present on Au wafer.

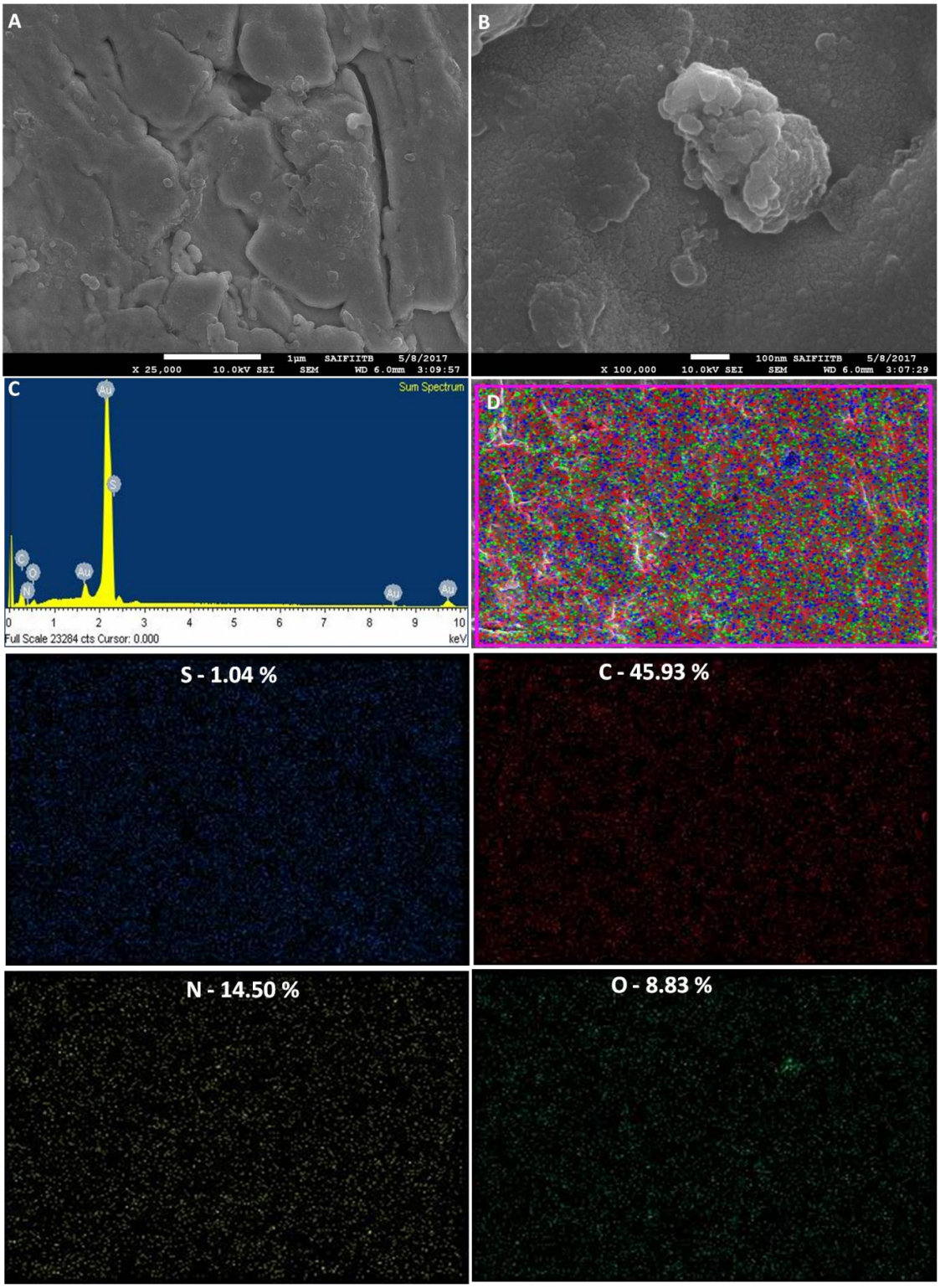

Figure S11: (A-B) SEM images of Tris-PDA electrode with Protein in PBS buffer (System II), C. EDS spectra and D. Elemental mapping showing the percentage of elements present on Au wafer.

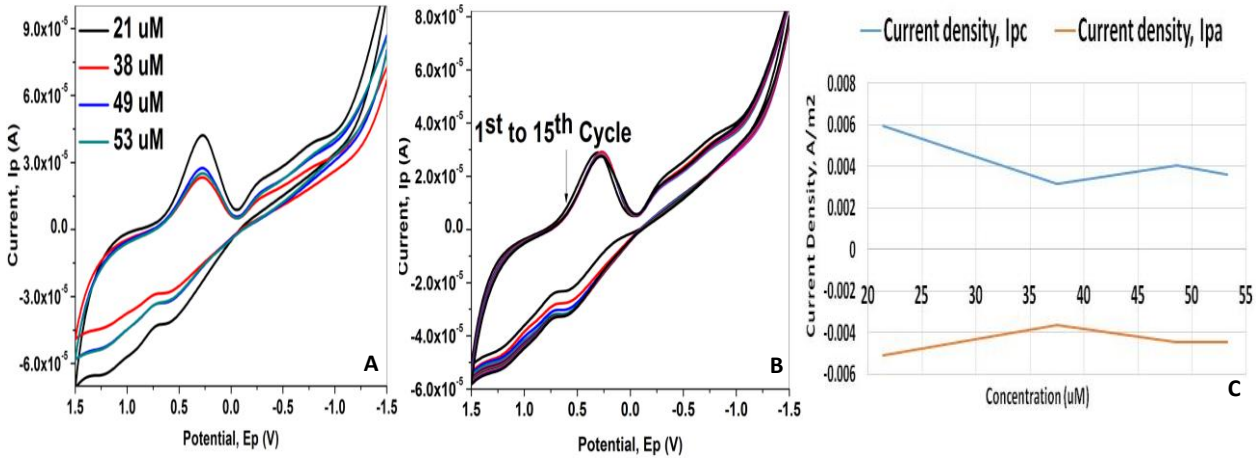

Figure S12:Cyclic voltammogram of Tris-PDA electrode with addition of A. different concentration of BSA at pH=7 and B. Repeated cycles on addition of 6 mL of 300 µM BSA AT pH 7 in Tris Buffer (System I), and C. change in current density with increase in concentration.

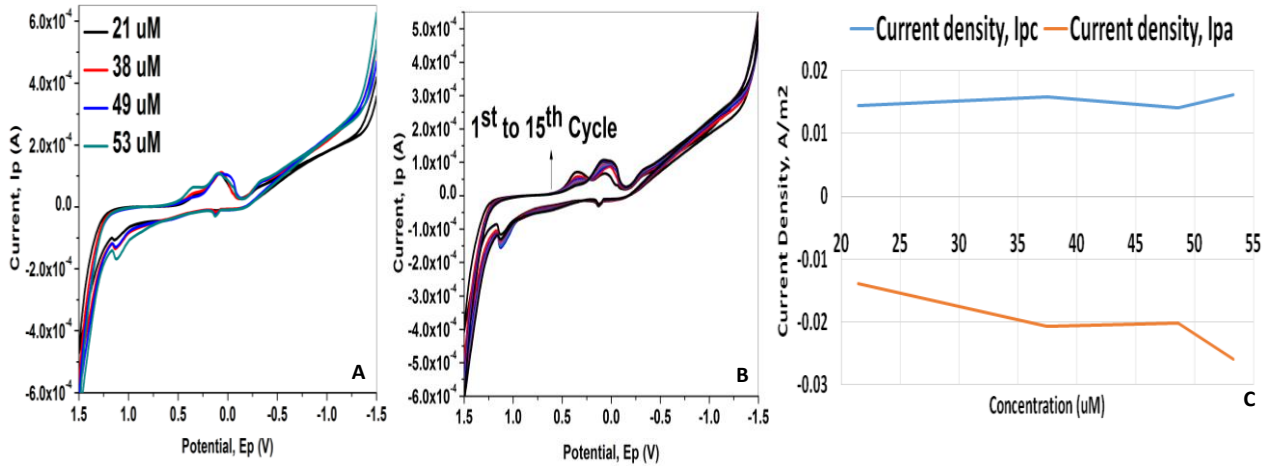

Figure S13:Cyclic voltammogram of Tris-PDA electrode with addition of A. different concentration of BSA at pH 7 and B. Repeated cycles on addition of 6 mL of 300 µM BSA at pH 7 in PBS buffer (System II), and C. change in current density with increase in concentration.

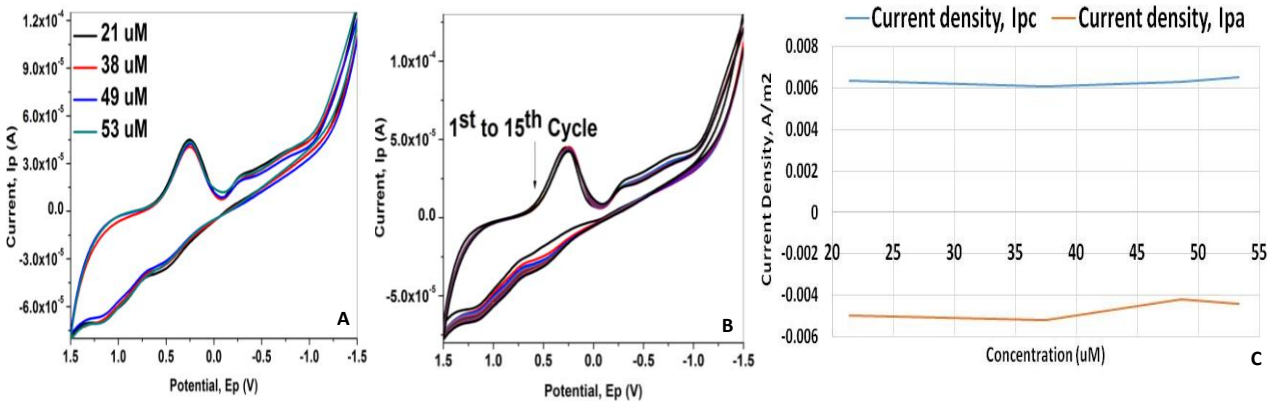

Figure S14:Cyclic voltammogram of PBS-PDA electrodewith addition of A. different concentration of BSA at pH 7, B. Repeated cycles on addition of 6 mL of 300 µM BSA at pH 7 in Tris buffer (System III)), and C. change in current density with increase in concentration.

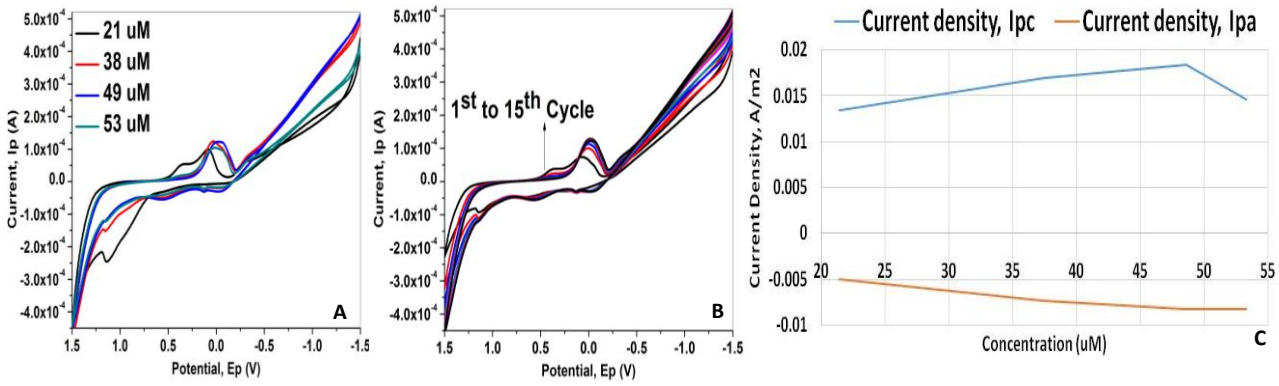

Figure S15:Cyclic voltammogram of PBS-PDA electrodewith addition of A. different concentration of BSA at pH 7, B. Repeated cycles on addition of 6 mL of 300 µM BSA at pH 7 in PBS buffer (System IV) , and C. change in current density with increase in concentration.

Cyclic Voltammetry

Polydopamine like eumelanin is semiconducting in nature and undergoes significant redox reactions when electrochemically challenged.[1]To evaluate the protein adsorption/desorption, CV responses of PBS-PDA and Tris-PDA coated electrodes were compared before and after addition of BSA solutions(300 µM in respective buffers). Briefly, the PDA coated electrodes were immersed in respective buffer solutions (Tris and PBS,5 mM, pH 7) and voltammogram were recorded. After this, cyclic voltammogram were recorded with the addition of different concentrations of BSA solutions. Typical voltammogram in absence and presence of BSA at pH7 in respective buffer solutions is shown in S16.Sharp reduction and oxidation peaks were observed in the voltammogram of polydopamine coated electrodes in absence of BSA. This redox behaviour shows the conductive nature of the coatings, an important parameter for protein adsorption studies.

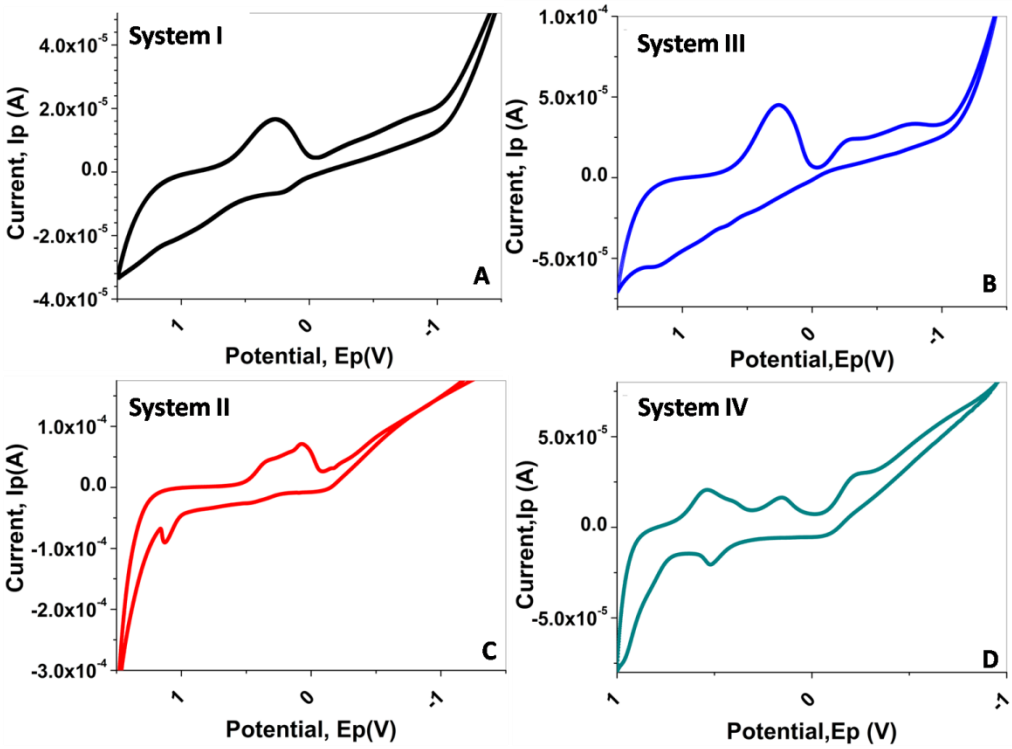

Figure S16: Cyclic voltammogram of polydopamine modified electrode before the addition of protein. (Systems I-IV are defined in Table-2)

It's interesting to note that irrespective of type of PDA coatings (Tris-PDA or PBS-PDA), electrolyte buffers show their distinct signatures in the cyclic voltammogram displaying characteristic shape and nature. The CV of system-III (defined in Table-2) reveals significant increase in current (Icp = 4.6 × 10^{-5} A) which is attributable to the electrochemical addition of the Tris nucleophile to the quinone groups by Schiff base/Michael addition thus, altering the electrochemical behaviour of polydopamine layers. This observation is supported by the fact that polydopamine undergoes covalent reaction with nitrogen containing nucleophiles present in polymerization buffers.[2, 3]

Upon addition of BSA (300 µM) the voltammogram of polydopamine coated electrodes reveals significant changes, with the peak current decreasing and peak potential shifting as shown in Fig. S17.

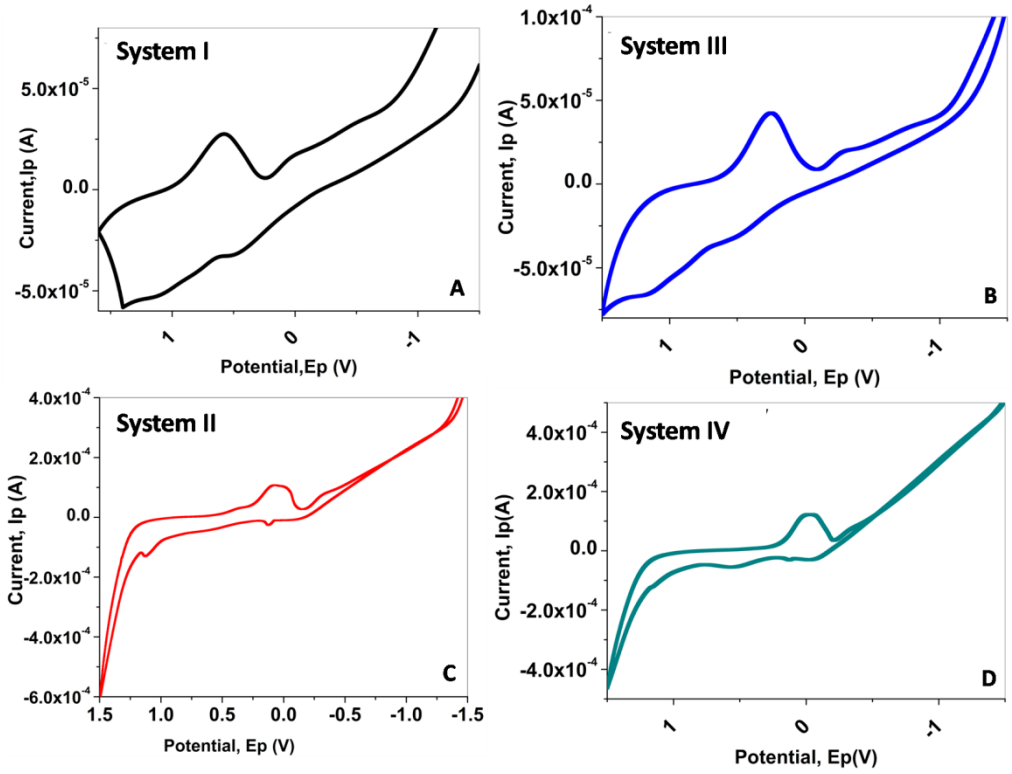

Figure S17: Cyclic voltammogram of polydopamine modified electrodes after addition of 300 µM protein solutions. (Systems I-IV are defined in Table-2)

These electrochemical changes in the current intensity and peak potential are attributable to the BSA adsorption on the polydopamine coated electrodes thus slowing down the electrochemical reactions. The electrochemical slowdown is larger when electrolyte is PBS buffer (System-II and System-IV) compared to the Tris buffer as electrolyte (System I and System-III). This is because of the blocking of the protein binding sites of polydopamine in presence of Tris which competes for the covalent binding sites (Schiff Base/Michael Addition Sites) on the polydopamine surfaces with nucleophilic groups of BSA. On the other hand, PBS buffer being devoid of nucleophilic groups don't competes with BSA for binding sites on polydopamine thus higher amount of BSA gets adsorbed. In other words, the protein binding sites on polydopamine remains accessible to BSA in PBS medium and gets blocked in Tris medium.

Since the solution pH plays an important role in protein adsorption, the CV was run with BSA solutions (6 mL, 300 µM in respective buffers) of different pH (pH4 -10). The voltammogram shows significant negative shift in reduction potential on increasing the pH to alkaline scale, pH 8 -10, which is attributed to overall negative charge of BSA (PI~5.0) and polydopamine layers (PI~9.7)[4] at higher pH.[5]The plot of current density vs. pH obtained after addition of BSA solution (Fig.S18A) shows that with increase in the pH the current density remains almost unchanged for System I and III where the protein binding sites in polydopamine were blocked by the nucleophilic Tris. However, for the system II and IV the current density decreases at the alkaline pH. At alkaline pH, there are greater

chances of protein binding to the polydopamine on account of deprotonation of nucleophilic (-NH_2 and –SH) groups. However, at highly alkaline pH the decrease in the current density can be explained on the basis of strong repulsive forces between highly negative polydopamine surfaces and BSA.

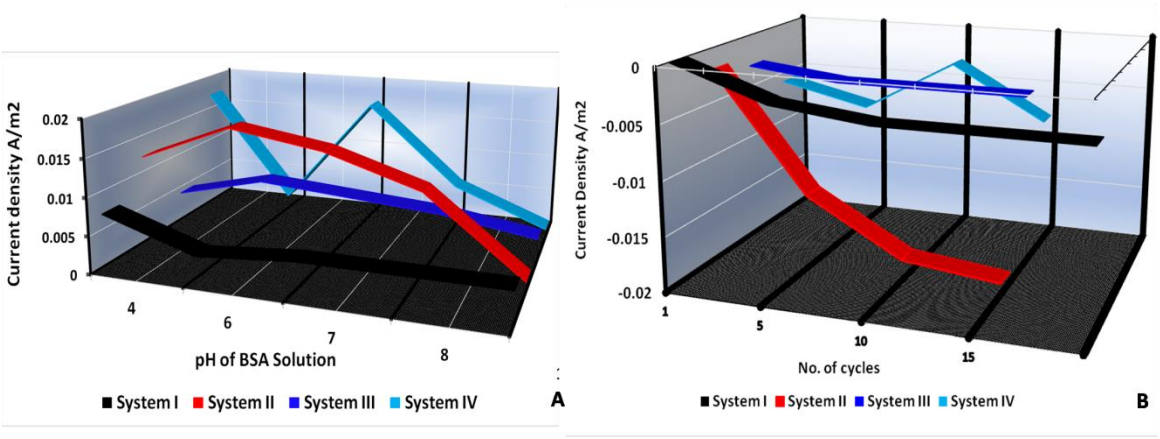

Figure S18: 3D spectra showing A. effect of pH and B. Number of cycles on current density using different electrodes in different buffers.

The repeated CV scans (15 cycles) with addition of BSA (6 mL, pH 7) shows no significant change in voltammogram position or shape (Fig. S12-S15) however, the current density shows linear changes for the system II and shows abrupt changes for system IV as shown in Fig. S18B. From the changes in the current density it can be inferred that system I and system III are practically resistant to the BSA binding as current density remains fairly unchanged which is because of Tris occupying the BSA binding sites on polydopamine. However, the system II and IV with easily available BSA binding sites shows changes in the current density with repetition of voltammetric scans on account of BSA binding/adsorbing onto the surface with each scan.

In order to prove this observation, CV was performed at different concentrations of the BSA solution. A current density vs. concentration plot as shown below in Fig.S19 suggests that system I and III restricts BSA adsorption/covalent binding and hence the change in current density is not significant when compared to the system II and IV where absence of nucleophilic Tris results in the higher concentration of BSA to access the available protein binding sites and thus covalently binding with the polydopamine and resulting in increase in the current density. It's worth mentioning that for system I and III the current don't increase or decrease much with addition of proteins which signify the protein adsorption resistance of the system I and III.

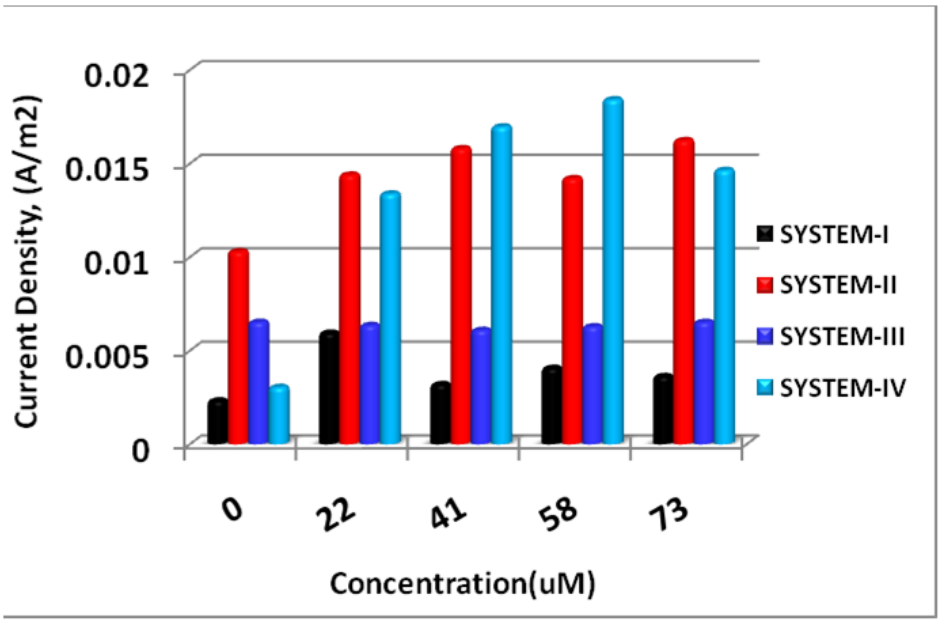

Figure S19: Bar Graph showing the change in current density on incremental addition of BSA solutions (300 µM) to electrochemical cell (system I-IV) at pH 7.4.

1. J. Wünsche, L. Cardenas, F. Rosei, F. Cicoira, R. Gauvin, C. F. O. Graeff, S. Poulin, A. Pezzella and C. Santato, *Advanced Functional Materials*, 2013, 23, 5591-5598.
2. N. F. Della Vecchia, R. Avolio, M. Alfè, M. E. Errico, A. Napolitano and M. d'Ischia, *Advanced Functional Materials*, 2013, 23, 1331-1340.
3. N. F. Della Vecchia, A. Luchini, A. Napolitano, G. D'Errico, G. Vitiello, N. Szekely, M. d'Ischia and L. Paduano, *Langmuir*, 2014, 30, 9811-9818.
4. K. Rurack and R. Martinez-Manez, *The Supramolecular Chemistry of Organic-Inorganic Hybrid Materials*, Wiley, 2010.
5. Y. J. Liu, C. Y. Lv and J. Yang, *Key Engineering Materials*, 2011, 467-469, 2024-2029.